Theory of reconstructive phase transitions in lyotropic complex fluids

B. Mettout,[1] P. Tolédano,[2,*] H. Vasseur,[3] and A. M. Figueiredo Neto[2]
[1]*Laboratoire de Physique des Solides, ESPCI, 10 rue Vauquelin, 75231 Paris Cedex, France*
[2]*Instituto de Física, Universidade de São Paulo, Caixa Postal 66318, 05315-970, São Paulo, São Paulo, Brazil*
[3]*Université de Picardie, 80.039 Amiens, France*
(Received 9 December 1996)

A phenomenological theory that describes the reconstructive transformations between ordered phases in lyotropic complex fluids is proposed. The symmetry-breaking order parameter of such transformations is assumed to be the undulation of the interfaces between the molecular aggregate regions and the solvent. It is shown to coincide with the first harmonics of a Fourier series expressing the form of the interfaces. In this framework, direct and reversed mesophases are shown to be related by a symmetry operation denominated the fluid-reversal symmetry. This underlying symmetry of the system clarifies a number of features of the phase diagrams of lyotropic complex fluids. The case of oriented interfaces, which corresponds to a tilting of the amphiphilic molecules on the interfaces, is also considered. [S1063-651X(97)09311-2]

PACS number(s): 64.70.Ja, 61.30.Gd

I. INTRODUCTION

There exist different types of phase transitions in lyotropic complex fluids. For the isotropic-nematic [1] and uniaxial-biaxial–nematic transitions [2] the shape of the molecular aggregates changes continuously with the external variables, i.e., the evolution in their forms corresponds to a homogeneous deformation. In this case the resulting equilibrium structures are generally related by group-subgroup relationships and the transitions between the corresponding phases are second order or slightly first order [3]. However, the most typical and widespread features of the phase diagrams of complex-fluid systems is the existence of *reconstructive phase transitions between ordered structures*: When varying the concentration of the surfactant and the temperature of these systems, the molecular aggregates exhibit discontinuous modifications in their geometry, with a drastic reorganization of the aggregates [4]. This leads to the formation of new structures across strongly first-order transitions surrounded by large polyphasic regions. The reconstructive character of these transitions is revealed by the absence of a group-subgroup relationship between the newly formed and the initial structures. This is the case, for instance, of the transitions between lamellar, cubic, and hexagonal mesophases, which are found in several lyotropic mixtures [5], polymer blends [6] and copolymer [7] systems, microemulsions [8], vesicles [9], biological membranes [10], etc.

Another specific property of the phase diagrams of complex fluids is the stabilization of *reversed* (inverted) mesophases [11]. In these mesophases the molecular aggregates and the solvent have approximately exchanged configurations with respect to the corresponding direct mesophases with the same basic geometry [5,11]. In lyotropic mixtures [5,11,12] in which reversed phases were first recognized, the occurrence of direct and reversed micellar structures has been comprehensively enumerated by Ekwall [11]. Thus the main classes (hexagonal, cubic, tetragonal, orthorhombic, etc.) of reversed phases exist in more distinct temperature-concentration ranges of the phase diagram than their direct analogs. Furthermore, the normal-to-reversed reconstructive transformation generally can be promoted by adding an additional hydrophilic (or less commonly lypophilic) compound to the binary system of amphiphiles and solvent. This transformation usually takes place through a sequence of intermediate mesophases, among which the lamellar phase is generally present [11,12].

A number of theoretical models have been proposed for the transitions between disordered mesophases [13,14] as well as for the transitions to ordered mesophases starting from the isotropic liquid [15,16]. However, up to now there has been no general theoretical approach to the reconstructive transitions that occur *between* ordered mesophases. On the other hand, there has been no attempt to explain theoretically the stability of reversed mesophases and their connections with the corresponding direct phases.

The aim of this article is to propose a unifying phenomenological model of reconstructive transitions between ordered mesophases in lyotropic complex fluids, which includes the description of the mutual relationship between the direct and reversed phases. More precisely, we will show through an illustrative example of the lamellar-tetragonal transition that the transitions between direct phases (Sec. II) and between the direct phases and their reversed analogs (Sec. III) can be obtained using a single symmetry-breaking order parameter that consists in the *periodic undulation of the interfaces* between the molecular aggregates and the solvent. In this description we will assume that the amphiphilic (sticklike) molecules are orthogonal, on average, to the interfaces. The more seldom case, which occurs when the molecules are tilted with respect to the interfaces, i.e., the case of *oriented interfaces*, will be considered in Sec. IV. It will be shown to relate to another irreducible degree of freedom associated with the assumed parent symmetry. In Sec. V the theoretical predictions of the model will be discussed and shown to clarify some features of the phase diagrams of a number of lyotropic systems. We conclude briefly in Sec. VI.

*On leave from the University of Picardie, Amiens, France.

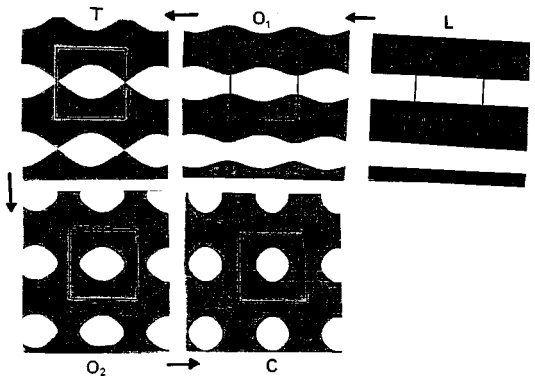

FIG. 1. Sequence of mesophases exhibiting the lamellar (L), intermediate (O_1,O_2), and tetragonal (C) phases. T denotes a topological transition.

II. TWO-DIMENSIONAL MODEL OF THE LAMELLAR-TETRAGONAL RECONSTRUCTIVE TRANSITION

A. Symmetry aspects of the model

Let us introduce the basic features of our model through a two-dimensional representation of the lamellar-tetragonal transformation in a system of amphiphiles in solution. Each equilibrium state is assumed to be formed by an assembly of two types of regions, denoted M and W, separated by interfaces and corresponding, respectively, to the molecular aggregates and to the solvent. Figure 1 illustrates one of the possible sequences of mesophases assumed in our approach, decomposing the successive steps of the transformation between the lamellar and tetragonal phases in the plane perpendicular to the lamellae. In agreement with the current theoretical [17,18] and experimental [19,20] descriptions of the instabilities in ordered mesophases, one can see that the symmetry-breaking mechanism inducing the reorganization of the mesophases consists in a periodic undulation of the interfaces when varying the concentration of surfactant or the temperature. Note that the lamellar (L) -tetragonal (C) transformation takes place across two types (''connected'' O_1 and ''disconnected'' O_2) of intermediate mesophases, which are separated by a *topological transition* [21], denoted T in Fig. 1. This transition occurs between phases of identical symmetries having a different topology of the surfaces limiting the molecular aggregates and the solvent.

Figure 2 represents another more complete sequence (cycle) of transformations that includes four orientational and translational *domains* of the L, C, O_1, and O_2 phases. Two distinct domains of the same mesophase transform into each other by combinations of a fourfold rotation with the discrete translations ($a/2$,0), (0,$a/2$) ,and ($a/2$,$a/2$) corresponding to half of the undulation periods along the x and y axes and their diagonal, respectively. a is the side of the square in Fig. 1.

In order to formalize the transformation processes represented in Figs. 1 and 2 one can restrict them to the (x,y) plane and write the equation of the interfaces in two dimensions as $\Psi(x,y)=0$. Ψ is assumed to be *positive* in the M regions and *negative* in the W regions. The minimal two-dimensional space group that contains all the symmetry operations leaving invariant the L, C, O_1, and O_2 phases (and their different domains) is

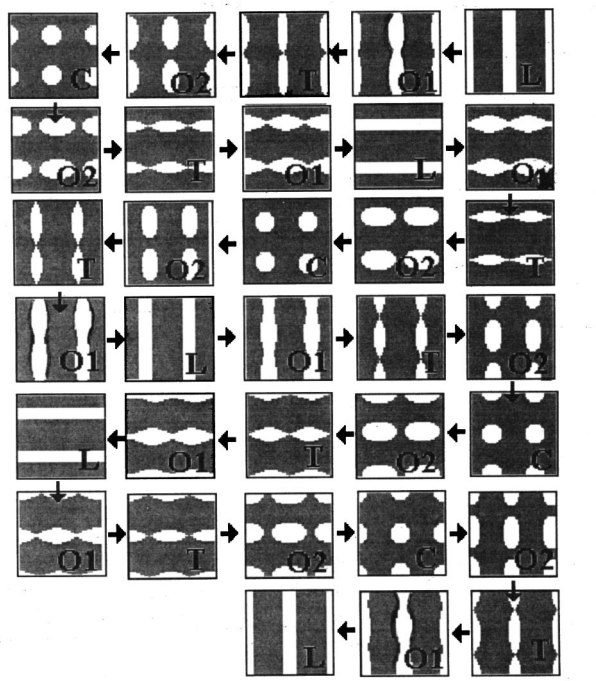

FIG. 2. Sequence of mesophases forming a cycle that includes four distinct domains of the L, C, O_1, and O_2 phases.

$$G_0=C_{4v}\times\Re^2, \tag{1}$$

where $\Re^2$ denotes the group of continuous translations in the (x,y) plane. G_0 is the minimal symmetry group that allows one to describe the lamellar-tetragonal transformation and is not *a priori* associated with a concrete structure. It will be assumed to correspond to the parent symmetry, denoted $\wp$, for the set of L, C, O_1, and O_2 phases. Restricted to a single domain (Fig. 1), the mesophases possess the symmetry groups:

$$\begin{aligned} &L{:}C_{2v}\times,(\Re_x,Z_y),\\ &C{:}C_{4v}\times(Z_x,Z_y),\\ &(O_1,O_2){:}C_{2v}\times(Z_x,Z_y), \end{aligned} \tag{2}$$

where the Schoenflies notation is used for the point-group symmetries and $\Re_x,Z_x,Z_y$ denote, respectively, a continuous translation along x and discrete translations along x and y.

Since all the phases are periodic, with at least one of the tetragonal discrete translations $Z_x=(a,0)$ and $Z_y=(0,a)$, $\Psi(x,y)$ can be developed in Fourier series as

$$\Psi(x,y)=\sum_{n,p=-\infty}^{+\infty}\Psi_{np}e^{2i\pi[(nx+py)/a]}, \tag{3}$$

where n and p are integers. One can show (the Appendix) that the coefficients of the first harmonics of this series, $\Psi_{10},\Psi_{01},\Psi_{\bar{1}0}=\Psi_{10}^*$ and $\Psi_{0\bar{1}}=\Psi_{01}^*$, form the basis of a four-dimensional irreducible representation of G_0, denoted

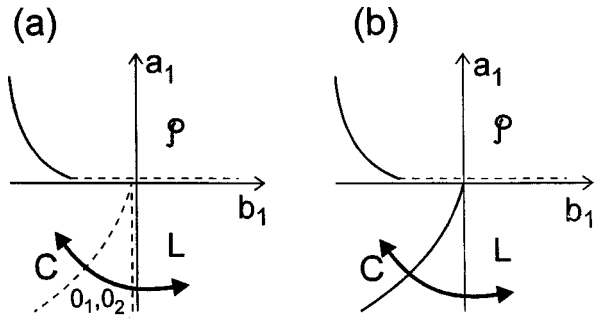

FIG. 3. Theoretical phase diagram associated with the Landau expansion (5) truncated at the sixth degree, in the plane of the phenomenological coefficients (a_1,b_1). $\wp$ denotes the parent phase of symmetry G_0. The double-headed arrow indicates the thermodynamic path followed in Fig. 1. Dashed and full lines are, respectively, second-order and first-order transitions lines. (a) $c_{12}<0$ and (b) $c_{12}>0$.

Γ_1. We will now demonstrate that Γ_1 induces, for different equilibrium values of the preceding coefficients, the different phases pertaining to the sequence of Fig. 1. In other words, these coefficients will be shown to represent *the four components of the order parameter describing the transitions between the L, C, O_1, and O_2 phases*.

Let us write $\Psi_{10}=\rho_1 e^{i\theta_1}$, and $\Psi_{01}=\rho_2 e^{i\theta_2}$. Since G_0 is a group depending on two continuous parameters $(\Re_x)$ and $(\Re_y)$, θ_1 and θ_2 are ''Goldstone'' variables, i.e., their shift does not modify the geometry of the phases but only displaces them globally in space, as can be foreseen in Fig. 2. Hence ρ_1 and ρ_2 represent the two *effective* components of the order parameter transforming as Γ_1. From the set of matrices expressing Γ_1 one can construct, as shown in the Appendix, two independent basic invariants

$$I_1=\rho_1^2+\rho_2^2, \quad I_2=\rho_1^2\rho_2^2, \tag{4}$$

which constitute the rational basis of integrity [22] of Γ_1. Therefore, the order-parameter expansion that transforms as Γ_1 has the general form

$$\mathcal{F}(\rho_1,\rho_2)=a_1I_1+a_2I_1^2+a_3I_1^3+\cdots+b_1I_2+b_2I_2^2+\cdots + c_{12}I_1I_2\cdots. \tag{5}$$

Minimization of $\mathcal{F}$ with respect to ρ_1 and ρ_2 yields three stable states, the symmetries of which are the subgroups of G_0, given by Eq. (2): For $\rho_1\neq 0$ and $\rho_2=0$ (or, equivalently, $\rho_1=0$ and $\rho_2\neq 0$) the L phase is stabilized. For $\rho_1=\rho_2\neq 0$, one obtains the C phase. The intermediate O_1 and O_2 phases correspond to $\rho_1\neq\rho_2\neq 0$. Figure 3 represents the theoretical phase diagrams associated with the expansion (5) when truncated at the sixth degree in ρ_1 and ρ_2, in the plane (a_1, b_1) of the phenomenological coefficients. Assuming a linear dependence of a_1 and b_1 as functions of the concentration c and the temperature T allows one to deduce the c-T phase diagram from the (a_1, b_1) phase diagram by a *linear* transformation that preserves the topology shown in Fig. 3. One can see that the L-C transition takes place either across the (O_1,O_2) phase, through two second-order transition lines [Fig. 3(a)], or across a first-order transition line [Fig. 3(b)] depending on the sign of the coefficient c_{12}. Note that these

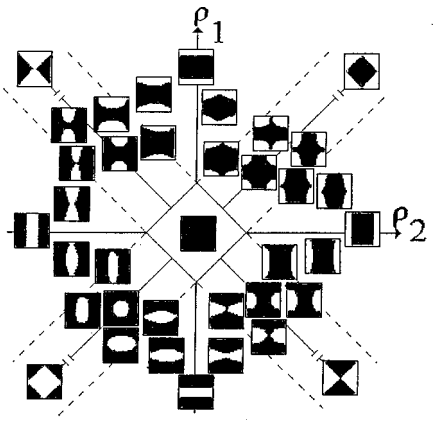

FIG. 4. Distribution of the mesophases of Fig. 2 in the order-parameter space.

phase diagrams have a physical meaning only for $a_1<0$ since in our approach the parent $\wp$ symmetry does not correspond to a stable state. Note also that the O_1 and O_2 states do not have separated regions of stability, i.e., the topological O_1-O_2 transition is not taken into account by a model based on the sole expansion (5).

The preceding deficiencies actually reveal the insufficiency of the standard Landau approach for describing reconstructive transitions. In the present case the phenomenological approach has to be completed by using the equation providing the form of the interfaces. Considering only the first harmonics in Eq. (3), i.e., taking into account exclusively the components of the symmetry-breaking order parameter, one can write this equation in the form

$$\Psi(x,y)=\Psi_{00}+\rho_1\cos\left(\frac{2\pi x}{a}\right)+\rho_2\cos\left(\frac{2\pi y}{a}\right)=0, \tag{6}$$

where the conditions $\theta_1=\theta_2=0,\pi$ have been taken into account.

Equations (5) and (6) allow us to describe the full distribution of stable states and the corresponding transitions between them as represented in Fig. 4, in the order-parameter space $\varepsilon=(\rho_1,\rho_2)$. Figure 4 reveals the following.

(i) Four domains of the L phase are located on the axes of ε space and the domains of the C phase on its diagonals. The general directions of ε space correspond to the stability regions of the O_1 and O_2 phases.

(ii) The interior of the central square in Fig. 4, which is defined by $|\rho_1\pm\rho_2|<1$, is excluded from the ε space since it corresponds to a phase formed exclusively by molecular aggregates or by the solvent, which possesses an isotropic symmetry.

(iii) The topological transitions take place between O_1 and O_2 along the directions prolongating the sides of the central square. These directions are defined by the equations $|\rho_2\pm\rho_1|=\pm 1$. Figure 4 reveals also that other topological transitions take place for *infinite* values of $|\rho_1|$ and $|\rho_2|$, between two types (disconnected and connected) of tetragonal phases, in the directions of the diagonals. Figure 5 shows the change in configuration of the M and W regions for this type of topological transition in the (ρ_1,ρ_1) direction. On can see that the transition occurs for an equal concentration

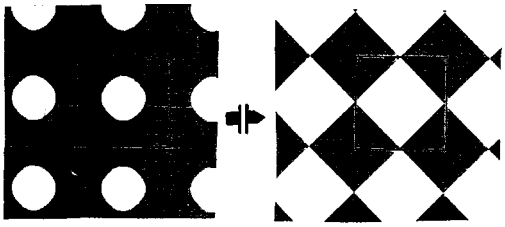

FIG. 5. Change in configuration of the M and W regions corresponding to the topological transition taking place for infinite values of ρ_1 and ρ_2 in the directions of the diagonals of the (ρ_1,ρ_2) plane.

of molecular aggregates and solvent, i.e., when the M and W regions occupy equal surfaces.

B. Effective thermodynamic potential

As illustrated by Figs. 1, 2, 4, and 5, the concentration c of molecular aggregates in solvent is an essential variational parameter for the evolution and stabilization of the mesophases. The suitable thermodynamic potential accounting for the evolution of concentration-dependent (open) systems should contain explicitly the concentration c expressed in terms of the order-parameter components. The dependence of c on ρ_1 and ρ_2 can be obtained by calculating the ratio of the surface S_M corresponding to an M region with respect to a constant total surface S containing the M and W regions. One can take, for example, $S=a^2$, which is the surface of the squares indicated in Fig. 1. Hence, as shown in Fig. 6, the concentration of molecular aggregates is defined by

$$c=\frac{S_M}{S}=\frac{1}{(a/2)^2}\int_0^{a/2}x(y)dy,$$

where $x(y)$ is deduced from Eq. (6):

$$x(y)=\frac{a}{2\pi}\arccos\left\{-\frac{1}{\rho_1}\left[1+\rho_2\cos\left(\frac{2\pi y}{a}\right)\right]\right\}.$$

One finds

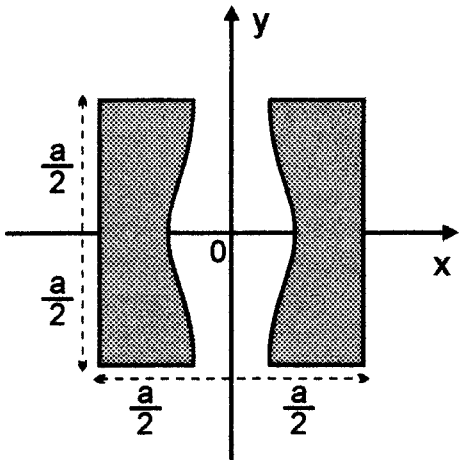

FIG. 6. Unit cell used for the calculation of the concentration $c(\rho_1,\rho_2)$ given by Eq. (7).

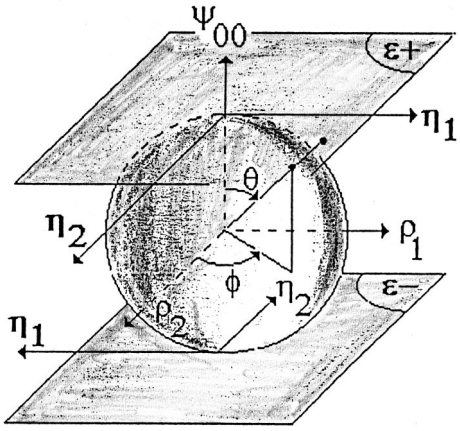

FIG. 7. Schematic representation on the order-parameter space ε, split into two sheets ε^+ and ε^-. The tangent sphere is used to express the order-parameter components in spherical coordinates (θ,φ).

$$c(\rho_1,\rho_2)=1-\frac{1}{\pi^2}\int_{-1}^{z_0}\arccos\left\{\frac{(1+\rho_2 z)}{\rho_1}\right\}(1-z^2)^{-1/2}dz, \tag{7}$$

with $z=\cos(2\pi y/a)$ and $z_0=(\rho_1-1)/\rho_2$ if $\rho_1-\rho_2>1$, whereas $z_0=1$ if $\rho_1-\rho_2<1$.

The thermodynamic potential (free energy) that allows one to describe the stable states of the system *at variable concentration and fixed difference between the chemical potentials* of the M and W regions can be written as

$$\Phi(\rho_1,\rho_2)=\mathcal{F}(\rho_1,\rho_2)-\tilde{c}(\rho_1,\rho_2)(\mu-\mu_0), \tag{8}$$

where μ and μ_0 are, respectively, the exchange chemical potentials between the M and W regions in the solution [23] and the exchange chemical potentials for the independent fluids at the same temperature and densities. $\tilde{c}=c-\frac{1}{2}$ is the reduced concentration. Note that in Eq. (8), $\mathcal{F}(\rho_1,\rho_2)$ has the meaning of the *interfacial energy* between the M and W regions and $-\tilde{c}(\mu-\mu_0)$ represents the contribution of the volumes of the fluids.

ρ_1 and ρ_2 are not convenient variables for working out the stable states of the system when c varies since they do not allow a continuous crossover at $c=\frac{1}{2}$ as their values become infinite for this concentration (see Figs. 4 and 5). This difficulty can be solved as follows: One can write $\Psi(x,y)$ in the form

$$\Psi(x,y)=\Psi_{00}\left[1+\eta_1\cos\left(\frac{2\pi x}{a}\right)+\eta_2\cos\left(\frac{2\pi y}{a}\right)\right], \tag{9}$$

where $\eta_1=\rho_1/\Psi_{00}$ and $\eta_2=\rho_2/\Psi_{00}$ transform as ρ_1 and ρ_2 since Ψ_{00} is a scalar. Figure 7 shows that the order-parameter space ε is split into two subspaces: ε^+ for $c>\frac{1}{2}$ and ε^- for $c<\frac{1}{2}$ (represented by two symmetrical sheets in Fig. 7), which correspond, respectively, to a positive and a negative sign of Ψ_{00}. This configuration is not practical since the crossover at $c=\frac{1}{2}$ from one subspace to another takes places for infinite values of ρ_1 and ρ_2. One can then

perform a mapping of the ε space on the sphere that is tangent to ε^+ and ε^- (see Fig. 7). This sphere is defined by

$$\Psi_{00}^2+\rho_1^2+\rho_2^2=1. \tag{10}$$

One can see that each couple $(\eta_1,\ \eta_2)$ coincides with *two* points of the sphere, of spherical coordinates $(\theta,\ \varphi)$ (one point in each hemisphere) with

$$\eta_1=\tan\theta\ \cos\varphi \qquad \eta_2=\tan\theta\ \sin\varphi. \tag{11}$$

As a consequence, the northern and southern hemispheres correspond to the equilibrium values of the order parameter for $c>\frac{1}{2}$ and $c<\frac{1}{2}$, respectively, while the equatorial plane symbolizes regions of equal concentrations for the *M* and *W* regions $t(c=\frac{1}{2})$, with a continuous crossover between the two hemispheres.

III. TRANSITIONS BETWEEN DIRECT AND REVERSED MESOPHASES: FLUID REVERSAL SYMMETRY

A. Fluid reversal symmetry

We will now show that the formalism introduced in the preceding section provides a natural description of the transitions between direct and reversed mesophases. Equation (9) expresses that a change in the sign of Ψ_{00} for identical values of η_1 and η_2 corresponds to the replacement of the *M* regions by the *W* regions or, in other words, *to the transformation from a direct to its reverse mesophase*. Accordingly, the stability of the phases is determined by *the reduced order parameter* (η_1,η_2) *and the sign of* Ψ_{00}. Hence the direct and reversed mesophases are obtained for the same values of η_1 and η_2, but in the different subspaces ε^+ and ε^-. Thus, if the distribution of mesophases shown in Fig. 4 takes place in the ε^+ subspace, an identical distribution holds for ε^- in which all *the mesophases are reversed*. This means that there exists a symmetry operation transforming a direct mesophase in its reversed analog. This operation, denoted *F*, which we term the *fluid-reversal symmetry*, is defined in the order-parameter space ε by

$$F(\Psi_{00},\eta_1,\eta_2)=(-\Psi_{00},\eta_1,\eta_2). \tag{12}$$

The effect of *F* corresponds in real space to the exchange of the respective volumes of surfactant and solvent, $F(V_M)=V_W$ or, equivalently, to a permutation of the concentration of the system from $c\geqslant\frac{1}{2}$ (the upper hemisphere in Fig. 7) to $F(c)=1-c\leqslant\frac{1}{2}$ (the lower hemisphere). Note that *F* has the property to commute with the space-symmetry operations of the system and that F_0F is an identity.

In the example considered in Sec. II the fluid has been assumed to be different on the two sides of an interface. Therefore, the *F* symmetry should in this case be at the utmost an aproximate symmetry since the interface should be spontaneously curved towards a preferential side due to the different interactions between the fluids and the surface. However, one can make the symmetry close to an exact symmetry by adding, for example, a third component, which may change the spontaneous curvature of the interfaces. In any case, the approximate nature of the fluid reversal symmetry does not preclude its influence on the phase diagram in which the mesophase are inserted. This will be made more clear by considering the effect of *F* on the thermodynamic potential Φ given by Eq. (8) and expressed in spherical coordinates.

In order to work out $\Phi(\theta,\varphi)$ one can use the following method. One searches for the more general function $\mathcal{F}(\theta,\varphi)$ invariant by G_0 (and eventually by *F*) that can be developed in a Fourier series of the variables θ and φ, i.e., in powers of the functions $a=e^{i\theta}$, $b=e^{-i\theta}$, $c=e^{i\varphi}$, and $d=e^{-i\varphi}$. These functions constitute the four components of the (nonlinear) order parameter. The corresponding curved manifold (from which the origin $a=b=c=d=0$ is excluded) obeys the constraints $|a|=|b|=|c|=|d|=1$, $ab=1$, and $cd=1$ relating the four functions. These constraints and the transformation properties of the functions by G_0 (and eventually by *F*) allow an explicit determination of the invariants I_1 and I_2 as functions of θ and φ. In the present case one can make use of the following practical considerations.

(i) $\mathcal{F}(\theta,\varphi)$ can be deduced from $\mathcal{F}(\rho_1,\rho_2)$ by a nonlinear singular transformation of the invariants I_1,I_2: $[I_1(\rho_1,\rho_2),\ I_2(\rho_1,\ \rho_2)]\rightarrow[I_1'(\theta,\varphi),\ I_2'(\theta,\varphi)]$, that is, a transformation that does not induce new singularities and preserves the symmetry of the irreducible representation Γ_1. If these conditions are fulfilled, the simplest form can be taken for $I_1'(\theta,\varphi)$ and $I_2'(\theta,\varphi)$.

(ii) *F* acts on the spherical coordinates (θ,φ) as $F(\theta,\varphi)\rightarrow(\pi-\theta,\pi+\varphi)$. Hence η_1 and η_2, as expressed by Eq. (11), are invariant by *F*, as well as the invariants $I_1=\tan^2\theta$ and $I_2=\tan^2\theta\sin^2 2\varphi$. Therefore $\mathcal{F}(\theta,\varphi)$ deduced from Eq. (5) is also invariant by $\mathcal{F}$. Following the preceding remarks, one can take the simplest invariants $I_1'=\cos^2\theta$ and $I_2'=\sin^2 2\varphi$, which possess the same transformational properties as $(I_1,\ I_2)$ with respect to G_0 and *F*. Thus the interfacial energy takes the form

$$\mathcal{F}(\theta,\varphi)=a_1\cos^2\theta+a_2\cos^4\theta+\cdots+b_1\sin^2 2\varphi+\cdots +c_{12}\cos^2\theta\sin^2 2\varphi+\cdots. \tag{13}$$

For a system noninvariant by *F*, but invariant by G_0, one can use the set of basic invariants $I_1''=\cos\theta$ and $I_2'=\sin^2 2\varphi$ since $F(\cos\theta)=-\cos\theta$. The form of $\mathcal{F}(\theta,\varphi)$ is, in this case,

$$\mathcal{F}(\theta,\varphi)=a_1\cos\theta+a_2\cos^2\theta+\cdots+b_1\sin^2 2\varphi+\cdots +c_{12}\cos\theta\sin^2 2\varphi+\cdots. \tag{14}$$

Note that the periodic functions (13) and (14) are defined for any values of $0\leqslant\theta\leqslant\pi$ and $0\leqslant\varphi\leqslant 2\pi$, namely, for unnecessary small values of the trigonometric functions $\cos\theta$ and $\sin 2\varphi$.

(iii) For the concentration *c* given by Eq. (7), one has by definition $F(c)=1-c$. Therefore, the reduced concentration $\tilde{c}$ is antisymmetric with respect to F: $F(\tilde{c})=F(c)-\frac{1}{2}=\frac{1}{2}-c=-\tilde{c}$. $\tilde{c}$ can actually be written under the general form

$$\tilde{c}=\cos(\theta)G(I_1',I_2'), \tag{15}$$

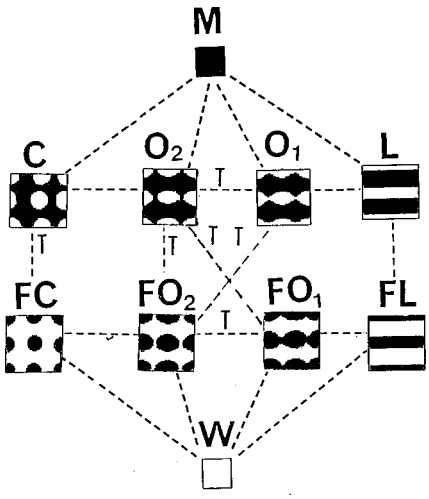

FIG. 8. Symmetry connections between the mesophases in the ε^+ (upper part of the figure) and ε^- (lower part) order-parameter subspaces for an F-noninvariant system. T denotes a topological transition.

where G is an integral function depending exclusively on I_1' and I_2'. We will now consider separately the phase diagrams associated with systems noninvariant and invariant, respectively, by F.

B. F-noninvariant systems

The noninvariance of a system under the symmetry operation F is the rule when the interfaces are spontaneously curved towards the M or W regions or when the two sides of the interfaces are inequivalent. Minimizing the free enery $\Phi(\theta,\varphi)=\mathcal{F}(\theta,\varphi)-\tilde{c}(\theta,\varphi)(\mu-\mu_0)$ with respect to θ and φ, where $\mathcal{F}(\theta,\varphi)$ and $\tilde{c}(\theta,\varphi)$ are expressed by Eqs. (14) and (15), respectively, one finds the four stable phases L, C, O_1, and O_2, in agreement with the results obtained by the minimization of $\mathcal{F}(\rho_1,\rho_2)$ with respect to ρ_1 and ρ_2 (Sec. II). The phases are stabilized for any values of θ and for the following equilibrium values of φ:

$$L:\left(\varphi=0,\frac{\pi}{2}\right),$$

$$C:\left(\varphi=\frac{\pi}{4}\right), \tag{16}$$

$$(O_1,O_2):\left(\varphi\neq 0,\frac{\pi}{4},\frac{\pi}{2}\right).$$

Note that the value $\theta=0$ corresponds to a point belonging to the central square in (ρ_1,ρ_2) space, which is excluded from the physical space.

The upper part of Fig. 8 illustrates the symmetry connections between the stable mesophases in the ε^+ subspace $(0\leqslant\theta\leqslant\pi/2)$, whereas the lower part of the figure shows the analogous configuration for the reversed mesophases in ε^- $(\pi/2\leqslant\theta\leqslant\pi)$. Here the reversed mesophases are distinct phases (except for the L and O_2 phases) resulting from the application of F, which is not a symmetry operation of the system. As indicated in Fig. 8, the transition between a direct phase and its reversed analog can be of the topological type. This can be viewed in Fig. 9, which represents the location of the direct and reversed phases in the (I_1'',I_2') space. The dashed lines in this figure are lines of topological transitions. The figure also reveals the existence of a continuous crossover between the L phase and a reversed-F L phase.

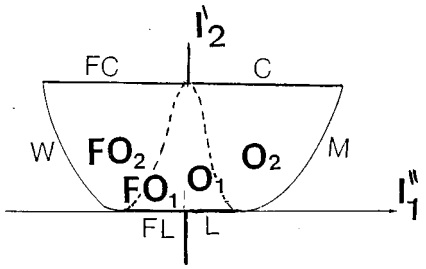

FIG. 9. Location of the mesophases of Fig. 8 in the space (I_1'', I_2'). The dashed line denotes a topological transition line.

Direct and reversed mesophases should not be present simultaneously in the phase diagrams of F-noninvariant systems. However, there may exist some exceptions. In this case the two phases should be located symmetrically with respect to $c=\frac{1}{2}$. However, since they are distinct phases, their shape should be asymmetrical with respect to the preceding value. A possible illustrative example of an F-noninvariant system is the decaoxyethylene-glycol monolauryl-ether-oleic acid-water system [11] in which the direct and reversed cubic phases occur, respectively, around the concentrations $c=0.43$ and 0.58 for low and middle concentrations of oleic acid. The phases are located symmetrically with respect to $c=\frac{1}{2}$, but the transition lines surrounding the phases are asymmetric with respect to the preceding value. Other possible examples of F-noninvariant systems are proposed in Sec. V.

C. F-invariant systems

A system invariant by F has its interfaces indifferently spontaneously curved towards the M or the W regions, i.e., one may have eventually spontaneously planar interfaces. In addition, the two sides of the interfaces should be equivalent. Using the form of $\mathcal{F}(\theta,\varphi)$ given by Eq. (13) and the expression of $\tilde{c}(\theta,\varphi)$ given by Eq. (15), the minimization of $\Phi(\theta,\varphi)$ with respect to θ and φ yields eight possibly stable ordered mesophases. Their symmetries and interconnections are shown in Fig. 10. One can see that in addition to the L, C, O_1, and O_2 phases, one finds four additional mesophases denoted L^*, C^*, O_1^*, and O_2^*, which are obtained for fixed values of the angles φ *and* θ. Thus L^* corresponds to $\theta=\pi/2$, $\varphi=0,\pi/2$, C^* is stabilized for $\theta=\pi/2$, $\varphi=\pi/4$, and (O_1^*,O_2^*) are obtained for $\theta=\pi/2$ and $\varphi\neq 0,\pi/4,\pi/2$. These ''starred'' phases possess the remarkable property that *half of their symmetry operations are combined with* F. Their space groups are generated by the symmetry elements

$$L^*:\left[F\cdot\sigma,F\cdot\left(0,\frac{a}{2}\right)\right],$$

$$C^*:\left[F\cdot C_4,\sigma,F\cdot\sigma_d,F\cdot\left(\frac{a}{2},\frac{a}{2}\right)\right], \tag{17}$$

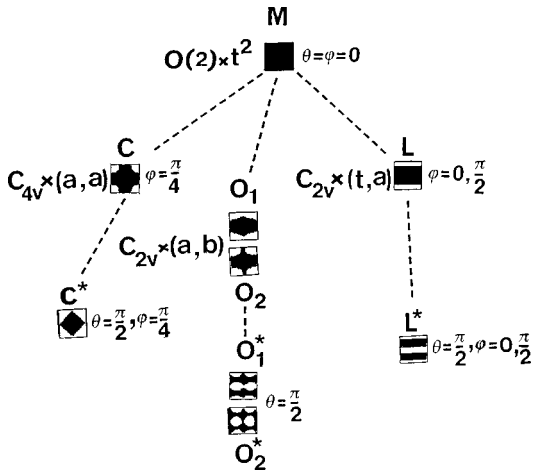

FIG. 10. Symmetry connections between the mesophases for an F-invariant system. The equilibrium values of θ and φ and the corresponding symmetry groups are given for the M, C, L, O_1, and O_2 phases. The symmetry groups of the starred phases C^*, L^*, O_1^*, and O_2^*, which are realized for $c=\frac{1}{2}$, are given in the text.

$$(O_1^*,O_2^*):\left[C_2,F\cdot\sigma,F\cdot\left(\frac{a}{2},\frac{b}{2}\right)\right],$$

where the standard crystallographic notation for the composition of symmetry operations is used for the planes (σ,σ_d) and axes (C_2,C_4). As shown in Fig. 10, this implies that the M and W regions occupy equal surfaces, i.e., the phases are stabilized for $c=\frac{1}{2}$. For this value of c the antisymmetric part $\tilde{c}$ of the potential $\Phi(\theta,\varphi)$ vanishes and Φ is fully invariant by F.

In an F-invariant system the direct and reversed mesophases correspond to *domains of the same equilibrium state*, transforming one into another by application of F. This property appears in Fig. 11, which represents the stable mesophases in $(I_1'\ I_2')$ space. The figure shows that the starred phases coincide with points or lines that limit, respectively, the lines and surfaces symbolizing the regions of stability of the L, C, O_1, and O_2 phases. Figure 12 shows a sequence of mesophases in which the reversed phases take place as the result of an enlargement of the M regions with respect to the W regions, in a progressive crossover from the northern (ε^+) to the southern (ε^-) hemispheres of the spherical order-parameter space going through the equatorial plane $(c=\frac{1}{2})$, which is the region in which the starred phases are defined.

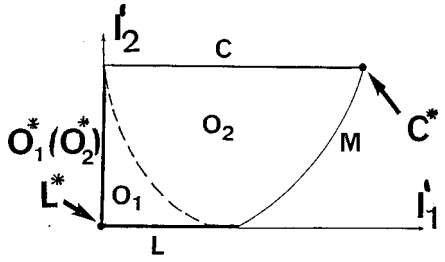

FIG. 11. Location of the mesophases classified in Fig. 10, in the space (I_1',I_2').

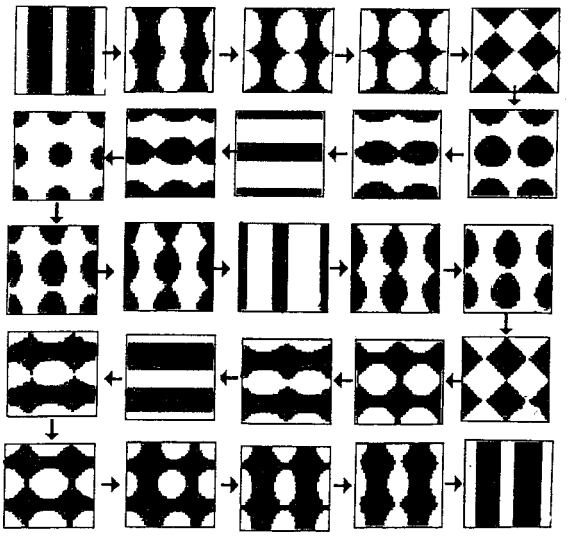

FIG. 12. Sequence of mesophases for an F-invariant system. The reversed phases take place in the same sequence as the direct phases as a result of an enlargement of the M regions.

In the phase diagram of F-invariant systems, the direct and reversed mesophases will be disclosed in distinct regions symmetrically located with respect to $c=\frac{1}{2}$. Since they correspond to the same equilibrium state, their phase boundaries should be symmetrical with respect to the preceding value. For example, in the sodium-caprylate decanol-water and sodium-caprylate-nonanol-water systems [11] the hexagonal direct (E) and reversed (F) mesophases take place around the water concentration $c=\frac{1}{2}$ for low and high concentrations of decanol or nonanol, respectively. Futhermore, in these systems the lines limiting the E and F phases are almost symmetric with respect to the preceding concentration. Other possible examples of F-invariant systems are described in Sec. V.

The preceding examples show that although the invariance by F can, in principle, be realized only in definite intervals of concentration, the conjunct stability of the direct and reversed phases can be enhanced by additional components that may extend the region of visibility of the phases. This remark holds also for the observation of the starred phases. For a system invariant by F one may *a priori* observe such phases only for a $c=\frac{1}{2}$ concentration. However, such a concentration can never be strictly realized, and since the starred phase appears as a *line* in the T-c phase diagram a transition between starred and unstarred phases should not, in principle, be observed. However, the existence of starred phases can be verified in the polyphasic regions that surround first-order transition lines. In these demixed regions it should be possible to observe phases corresponding to concentrations that differ from the nominal values associated with the phases surrounding the transition line. This property stems from the connection existing between the μ-T (chemical potential temperature) and c-T phase diagrams. In the μ-T phase diagrams the starred phases display stability surfaces that become lines in the c-T phase diagram. But there may exist in the μ-T phase diagrams starred-unstarred first-order transitions associated with demixed *regions* that should remain surfaces in the c-T phase diagrams. This property is still valid for systems that display only an approximate in-

variance by F, i.e., for which the noninvariant part of the potential $\mathcal{F}(\theta,\varphi)$ is small with respect to its invariant part. In this case one should observe in the μ-T plane either a continuous crossover or a first-order isostructural transition between two regions of unstarred phases corresponding to a small noninvariant part for the $\mathcal{F}(\theta,\varphi)$ potential.

In summary, it has been shown in this section that the existence of reversed mesophases in lyotropic complex fluids can be understood by considering an additional symmetry operation, the fluid-reversal symmetry F, which provides a classification of ordered mesophases. In particular, the existence of a different type of mesophase, in which half of the symmetry elements are combined with F, has been predicted. On the other hand, it has been suggested that the F symmetry, despite its approximate character, may influence the type of ordering existing in regions of the phase diagrams of some complex-fluid systems. Such considerations are strongly reminiscent of the influence of the exchange interaction on the property of magnetically ordered systems. This analogy helps to understand to what extent the approximate character of the F symmetry may eventually limit its influence on the observable properties of lyotropic systems. Thus, in the phenomenological approach to magnetic transitions [24], the thermodynamic potential is divided into two parts that reflect, respectively, the (isotropic) exchange interaction and the (anisotropic) relativistic interactions (spin-orbit, spin-spin, etc.). While the relativistic terms determine the magnetic symmetry of the phases, the exchange forces are mainly responsible for the type of magnetic ordering since they are several orders of magnitude larger than the relativistic forces.

In a similar way there exists a hierarchy of symmetries in complex fluids depending on the relative magnitude of the interactions: If the F-invariant part of the potential $\Phi(\theta,\varphi)$ is substantially larger than the F-noninvariant part, the properties of the system will reflect the action of the F symmetry. In this respect the existence in the same phase diagram of direct and their reversed mesophases and the symmetric location of these phases with respect to $c=\frac{1}{2}$ are, following our model, definite indications of the influence of the fluid-reversal symmetry.

IV. LYOTROPIC COMPLEX-FLUID SYSTEMS WITH ORIENTED INTERFACES

In Secs. II and III the amphiphilic molecules were implicitly assumed to be, on average, orthogonal to the interfaces. This actually corresponds to the most common configuration found among ordered mesophases in complex fluids. Figure 13 illustrates schematically this orthogonal configuration for the lamellar phase [Fig. 13(a)] for an undulated lamellar phase [Fig. 13(b)] and for the direct tetragonal [Fig. 13(c)] and reversed tetragonal [Fig. 13(d)] mesophases. However, in some cases, such as the $L_{\beta'}$ mesophase found in interacting lipid membranes [25–27], the molecules are *tilted* with respect to the surfaces, in a smectic-C type of configuration. Figure 14 shows two types of tilting that may occur for the amphiphilic molecules within a lamella, i.e., with the same orientation for the two molecular layers [Fig. 14(a)] or with a chevron-type ordering [Fig. 14(b)]. One can see in Fig. 14(a) that the surfaces determined by the heads of the amphiphiles

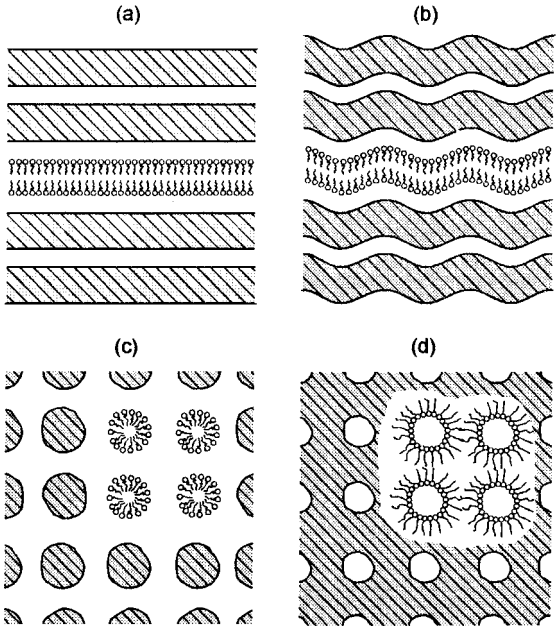

FIG. 13. Orthogonal configuration of the amphiphile molecules on the interfaces for (a) a lamellar phases, (b) an undulated lamellar phase, (c) a tetragonal phase, and (d) a reversed tetragonal phase.

possess an *orientation*, which is given by the direction of the projection of the molecular vectors on the interface.

The aim of the present section is to show that in the case of *oriented interfaces*, the phenomenological model developed in the previous sections applies differently and yields a number of specific properties for the corresponding systems.

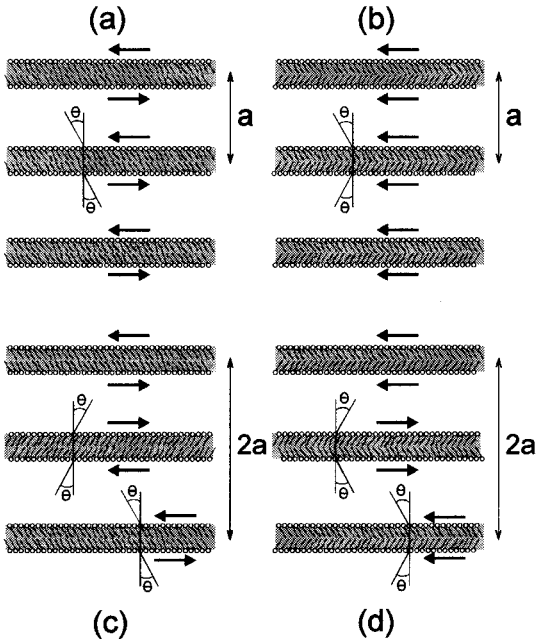

FIG. 14. Different types of tilting occurring for a lamellar phase with oriented interfaces (a) and (c) Opposed orientations for two consecutive interfaces of the M regions, with (a) a simple and (c) a double interlayer periodicity. (b) and (d) Identical orientations for two consecutive interfaces of the M regions with (b) a simple and (d) a double interlayer periodicity in the case of a chevron-type structure.

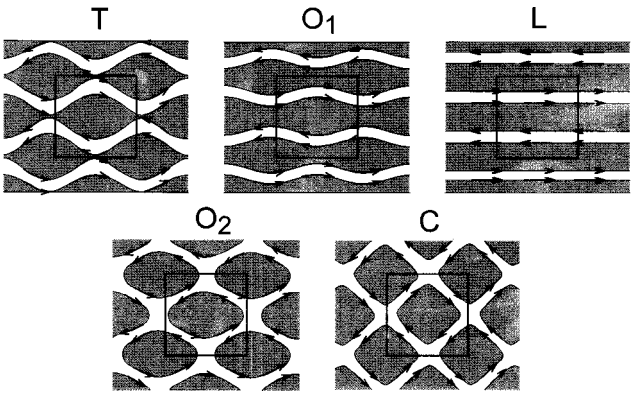

FIG. 15. Sequence of L, O_1, O_2, and C mesophases for the lamellar stacking of Fig. 14(c). The arrows denote the orientations of the interfaces.

In particular, the undulation mechanism that induces the lamellar-tetragonal transformation obeys constraints different from those for systems with ''orthogonal'' interfaces. In order to make this point clear we will first analyze in more detail the undulation mechanism used in Sec. II.

A. Symmetry-breaking undulation mechanisms

The undulation of the interfaces assumed in Fig. 1 displays the following properties: (i) Two neighboring surfaces limiting the same (M or W) region are dephased by π, and (ii) two consecutive M (or W) regions behave identically, i.e., they are in phase, ensuring a minimal periodicity (a) in the direction perpendicular to the interfaces. These two features are not arbitrary and represent necessary conditions for the sequence of phases shown in Fig. 1 to take place. Figure 13(b) illustrates, for example, the property that the absence of dephasing between two consecutive regions would not allow a symmetry-breaking mechanism giving rise to the tetragonal mesophase. Along the same line, the fact that the M and W regions play a symmetric role is also a necessary condition for the existence of the fluid-reversal symmetry.

A different situation occurs when the interfaces are oriented. It is easy to verify from the lamellar configurations shown in Figs. 14(a) and 14(b) that an identical orientation for two consecutive M (or W) regions excludes a phase opposition for two neighboring M and W regions. In order to obtain such a dephasing one has to double the periodicity ($2a$) in the direction perpendicular to the interfaces, i.e., to assume a lamellar configuration of the type represented in Fig. 14(c) or 14(d), in which two consecutive lamellae of the M regions exhibit opposed orientations of the molecules and interfaces. Note that in this case the M and W regions do not behave symmetrically. A consequence that will be shown hereafter is *the absence of F symmetry for systems with oriented interfaces*.

Figures 15 and 16 illustrate the undulation mechanisms corresponding, respectively, to the lamellar stackings represented in Figs. 14(c) and 14(d). They induce a sequence of phases that are labeled, by analogy with Fig. 1, L, O_1, O_2, and C. The micelles are formed after a topological transition (T) between the O_1 (connected) and O_2 (disconnected) mesophases. Note that in Fig. 15 two consecutive M regions undulate in phase opposition and two consecutive W regions

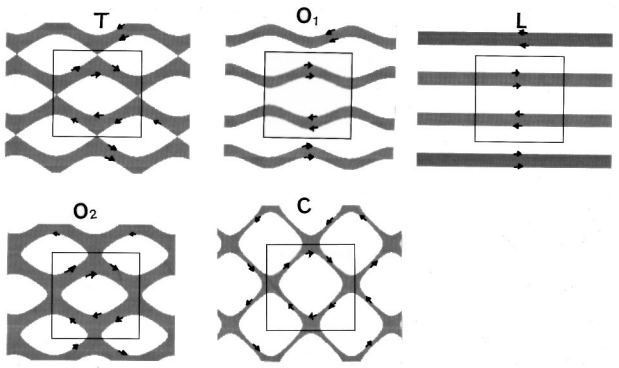

FIG. 16. Sequence of L, O_1, O_2, and C mesophases for the lamellar stacking of Fig. 14(d).

are in phase, whereas the reversed situation is found in Fig. 16. In other words, the undulation mechanisms assumed in these two figures are reciprocal and can be deduced from another by the permutation $M \leftrightarrow W$, i.e., by an F symmetry.

B. Field lines and oriented domains

While the position of the interfaces in the (x,y) plane is given by the equation $\Psi(x,y)=0$, the orientation of the interfaces can be expressed by two quantities: (i) the vector field $\vec{\Psi}(x,y)$, where the value of $\vec{\Psi}(x,y)$ on a given interface corresponds to the projection on this interface of the molecular vector, i.e., for a unit-molecular vector it measures the *tilt angle* with respect to the normal to the interfaces, and (ii) since there exists an infinite set of field lines for a given vector field $\vec{\Psi}$, one has to chose the field line on which $\vec{\Psi}$ is determined (see below) and represents the actual interface.

Since all the structures shown in the sequences of Figs. 15 and 16 are periodic, the two components Ψ_x and Ψ_y of $\vec{\Psi}(x,y)$ can be expanded in Fourier series

$$\Psi_x(x,y)=\sum_{n,p=-\infty}^{+\infty}\Psi_{np}^{x}e^{(2i\pi/a)(nx+py)},$$

$$\Psi_y(x,y)=\sum_{n,p=-\infty}^{+\infty}\Psi_{np}^{y}e^{(2i\pi/a)(nx+py)}. \tag{18}$$

Considerations similar to those developed in Sec. II for the scalar quantity $\Psi(x,y)$ lead to a simplified form for Ψ_x and Ψ_y. Namely, one considers the first harmonics in Eq. (18), which are $\Psi_{01}^{x},\Psi_{10}^{y},\Psi_{0\bar{1}}^{x}=\Psi_{01}^{x}{}^{*}$ and $\Psi_{\bar{1}0}^{y}=\Psi_{10}^{y}{}^{*}$. The preceding components span the other four-dimensional irreducible representation, denoted Γ_2, of the product group G_0 (see the Appendix). Then one writes $\Psi_{01}^{x}=\rho_1 e^{i\theta_1}$ and $\Psi_{10}^{y}=\rho_2 e^{i\theta_2}$, in which the Goldstone variables θ_1 and θ_2 can be assumed to be zero. This yields

$$\Psi_x=\rho_1\cos\frac{2\pi y}{a},\quad \Psi_y=\rho_2\cos\frac{2\pi x}{a}. \tag{19}$$

On the other hand, the equation of the field lines is

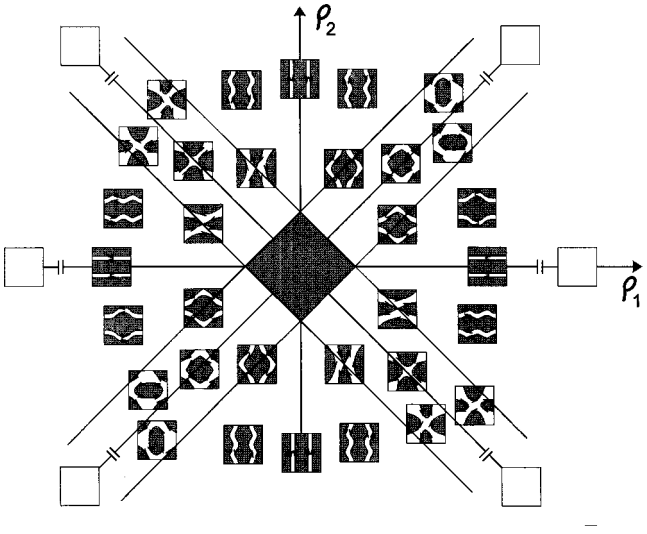

FIG. 17. Distribution of the mesophases with oriented interfaces, in the order-parameter space (ρ_1,ρ_2).

$$\rho_2 \sin\left(\frac{2\pi x}{a}\right) - \rho_1 \sin\left(\frac{2\pi y}{a}\right) = \pm k, \tag{20}$$

where the value of the constant k obeys the conditions $-(\rho_1+\rho_2) \leqslant k \leqslant \rho_1+\rho_2$. Note that the field lines corresponding to the same value of k but to opposite signs are oriented in opposite directions and determine the same M or W region. Therefore, the full set of stable structures and their orientations are determined by the values of ρ_1 and ρ_2 and by the absolute value of the constant k. Figure 17 shows the distribution and orientations of the stable mesophases in the order-parameter space (ρ_1,ρ_2) assuming the M and W configurations of Fig. 15. It reveals the following similarities and differences with respect to the ''scalar'' distribution of Fig. 4.

(i) The L phases are located on the axes of the (ρ_1,ρ_2) space, while the C phases are on the diagonals. The general directions correspond to the intermediate (O_1,O_2) mesophases. O_1 and O_2 are separated by lines of topological transitions that elongate the sides of the central square. Except for its borders, this square is excluded from the order-parameter space.

(ii) The M and W regions play a disymmetrical role, i.e., the W regions undulate in phase with opposed orientation for two consecutive W region, whereas two consecutive M regions are in phase opposition with opposed orientations: They are alternatively depending on the values of ρ_1 and ρ_2, swollen or contracted. Note, in this respect, that Figs. 15 and 16 represent two essentially different mechanisms (order parameters) that, however, are associated with the same irreducible representation (Γ_2). If only one mechanism is assumed, the disymmetry between the M and W regions forbids the existence of direct and reversed mesophases in the same system.

(iii) The permutation $(\rho_1,\rho_2) \rightarrow (-\rho_1,-\rho_2)$ reverses the orientation of the interfaces, whereas the permutations $(\rho_1,\rho_2) \rightarrow (\rho_1,-\rho_2)$ and $(\rho_1,\rho_2) \rightarrow (-\rho_1,\rho_2)$ correspond to a combination of glide planes with translations $(a,0)$ and $(0,a)$, respectively, therefore, the four domains that are stabilized for each mesophase in the order-parameter space

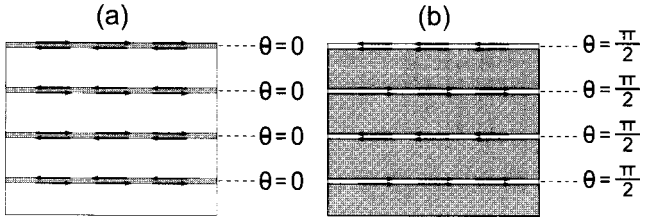

FIG. 18. Lamellar mesophases in the limit situations when (a) ρ_1 and ρ_2 become infinite along the axes of the order-parameter space $(c \rightarrow 0)$ and (b) ρ_1 and ρ_2 reach their limit values on the border $(\rho_1 = \rho_2 = 1)$ of the central square in Fig. 17 $(c \rightarrow 1)$.

(ρ_1,ρ_2) are deduced from each other by combinations of fourfold or twofold rotations and glide planes. Note that, at variance with the mesophase distribution shown in Fig. 4, the multiplication of ρ_1, ρ_2, and k by a positive constant λ *modifies the structure of the mesophases*, although the form of the interfaces remains unchanged. It results in a different value of $|\vec{k}|$, i.e., in a change of the tilt angle. In particular, at the limit $c=0$ $(k \rightarrow 0)$ opposed surfaces get closer and tend towards a zero field line [Fig. 18(a)] at which the molecular vectors become perpendicular to the interfaces $(\theta = 0)$: The W regions occupy the whole surface. This occurs for infinite values of ρ_1 and ρ_2 in Fig. 17. When $c \rightarrow 1 [k \rightarrow \pm(\rho_1 \pm \rho_2)]$ the tilt angle tends, on the contrary, to its maximal value $\theta = \pi/2$, which coincides with an orientation of the molecules parallel to the interfaces: The M region fully occupies the surface of the system [Fig. 18(b)]. This occurs at the border of the central square $(\rho_1 \pm \rho_2 = \pm k)$ in Fig. 17. We will now return to the thermodynamic considerations that had been used to determine the equilibrium values of the effective order-parameter components (ρ_1,ρ_2) in Fig. 17.

C. Symmetry of mesophases with oriented interfaces

The symmetry of the irreducible representation Γ_2 allows one to construct the same basic invariants I_1 and I_2 (see the Appendix) given by Eq. (4), which are constructed from Γ_1. However, one has to consider also the coupling between the form of the interfaces and their orientation. This can be foreseen from the equation of the interfaces, which, as deduced from Eq. (20), can be written

$$\left[\rho_2 \sin\left(\frac{2\pi x}{a}\right) - \rho_1 \sin\left(\frac{2\pi y}{a}\right)\right]^2 = k^2. \tag{21}$$

Therefore, the interfacial energy $\mathcal{F}(\rho_1,\rho_2,k)$ depends on the three invariants I_1, I_2, and $I_3 = k^2$. Its minimization yields the same equilibrium conditions as in the case of nonoriented surfaces: $L(\rho_1=0,\ \rho_2 \neq 0,$ or $\rho_1 \neq 0,\ \rho_2=0)$, $C(\rho_1=\rho_2 \neq 0)$, and (O_1,O_2) $(\rho_1 \neq \rho_2 \neq 0)$. However, the symmetries of these phases are different due to the orientation of the surfaces. One finds, using the standard notation of two-dimensional groups, the symmetry groups

$$\begin{aligned} L&: P2gm(R_x,Z_y), \\ C&: P4gm(Z_x,Z_y), \\ (O_1,O_2)&: P2gg(Z_x,Z_y), \end{aligned} \tag{22}$$

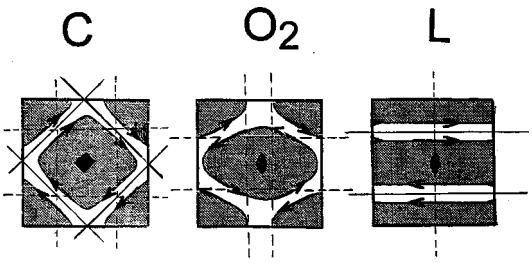

FIG. 19. Symmetry elements corresponding to the C, O_2, and L mesophases. The dashed lines represent glide planes.

which possess glide planes shown in Fig. 19.

Equation (21) can be expressed under the developed form

$$\rho_1\rho_2\left[\cos\frac{2\pi}{a}(x+y)-\cos\frac{2\pi}{a}(x-y)\right]+\frac{\rho_{1_2}}{2}\cos\left(\frac{4\pi y}{a}\right)+\frac{\rho_{2_2}}{2}\cos\left(\frac{4\pi x}{a}\right)+\left(\frac{\rho_1^2+\rho_2^2}{2}\right)=k^2. \tag{23}$$

This contains two harmonics of the Fourier series (3) corresponding to the wave vectors $\vec{a}^*\pm\vec{b}^*$ and $2\vec{a}^*$, where $\vec{a}^*$ and $\vec{b}^*$ are the reciprocal lattice vectors of $\vec{a}$ and $\vec{b}$. In other words, if the orientation of the surfaces are neglected in Fig. 15, the system will display the translations $(a/2,a/2)$ and $(a/2,-a/2)$ instead of (a,a). This reveals that the description of the form of the interfaces, for systems with oriented interfaces, requires one to consider at least two secondary scalar order parameters: an order-parameter spanned by the basic functions $e^{\pm 2i\pi/a^{(x+y)}}$ and $e^{\pm 2i\pi/a^{(x-y)}}$, which transforms as $\Gamma_1(a^*\pm b^*)$, and an order parameter spanned by the basic functions $e^{\pm 4i\pi x/a}$ and $e^{\pm 4i\pi y/a}$, which corresponds to the higher harmonics of wave vector $2\vec{a}^*$.

As in Sec. III, a realistic description of the phase diagrams containing ordered mesophases with oriented surfaces should make use of a thermodynamic potential containing explicitly the concentration c. A calculation analogous to the one leading to Eq. (7) gives here

$$c(\rho_1,\rho_2,k)=8\int_{(\omega_1-1)/\omega_2}^{0}\arccos\left\{\left(\frac{\omega_2 z+1}{\omega_1}\right)\right\}(1-z^2)^{-1/2}dz, \tag{24}$$

where $\omega_i=\rho_i/k$ (i = 1,2). Thus the full thermodynamic potential will have the general form

$$\Phi(\rho_1,\rho_2,k)=\mathcal{F}(\rho_1,\rho_2,k)-\tilde{c}(\rho_1,\rho_2,k)(\mu-\mu_0), \tag{25}$$

where $\tilde{c}$, μ, and μ_0 have the same meaning as in Eq. (8).

V. DISCUSSION

The phenomenological approach to reconstructive phase transitions in lyotropic complex fluids, developed in this article, has been introduced through a two-dimensional model of the lamellar-tetragonal transition. Extending the model in three dimensions increases the number of possible stable ordered mesophases and the variety of their symmetries as well as the types of possible transition sequences. For example, at the lamellar-cubic transition [28] the six-component relevant order parameter yields seven stable anisotropic mesophases corresponding to different continuous or discrete subgroups of $O_h\times\mathfrak{R}^3$. At the lamellar-hexagonal transition, one finds seven types of ordered mesophases [28] induced by a six-component order parameter transforming as an irreducible representation of the $C_{6v}\times\mathfrak{R}^2$ symmetry group. For these two examples, one can show that the essential results (the structure of the order-parameter space, existence of an underlying F symmetry for systems with nonoriented interfaces, topological properties of the phase diagrams, etc.) obtained for the lamellar-tetragonal case are still verified [29]. Therefore, in the following discussion it will be assumed that these results may provide a general qualitative interpretation of lyotropic systems.

The lamellar-tetragonal (L-C) transformation coincides with a realistic situation found in a number of ternary systems [11], such as sodium-caprylate–water + decanol, sodium-caprylate–water + caprylic acid, or decaethylene glycol monolauryl ether–water + oleic acid. In these systems the L and C phases identify, using the notation of Ekwall, the lamellar D and square C phases [11], respectively. The two preceding phases are separated by the so-called B phase, which is an undulated lamellar phase corresponding to the O_1 intermediate mesophase in our model. Analogously, the O_2 disconnected phase in Fig. 1 is similar to the R phase reported in potassium oleate water + p-xylene [11].

Let us verify the applicability of one of the main properties of the phase diagrams of lyotropic systems, i.e., the symmetric location with respect to $c=\frac{1}{2}$ of the direct and reversed mesophases and the eventual symmetry of their stability domains (in the case of F-invariant systems) with respect to the preceding value. Tables I and II summarize the corresponding data from Ekwall's review [11] for binary and ternary lyotropic systems respectively, in which one can find both a direct phase and its reversed analog. Table I shows that there exist only few binary systems fulfilling the preceding requirements. Furthermore, they contain only the direct L_1 and reversed L_2 micellar solutions, but not the two types of ordered mesophases simultaneously. One can note the following.

(i) The L_1 and L_2 regions are approximately symmetrical with respect to $c=\frac{1}{2}$ and occupy the extremities of the WM axis. An exact symmetrical location of L_1 and L_2 with respect to $c=\frac{1}{2}$ can be realized in a narrow interval of temperature, e.g., around 100°C for the aerosol OT-water system.

(ii) The lamellar D phase always occupies an intermediate region between the L_1 and L_2 regions. Its stabilization requires sometimes the addition of a few percent of a third component, as in Triton-x-100–water [11], where it appears for 5% of decanol, or in decaoxyethylene glycol-water [11], where one needs to add 10% oleic acid. In Emu-O_2-water the D phase fully occupies at 20°C, the intermediate region between L_1 and L_2. It would be of interest to verify in this region an eventual progressive change between the direct and reversed structures.

(iii) When the hexagonal (E) phase is stabilized, it occupies a region surrounding $c=\frac{1}{2}$. In Triton-x-100–water E is almost symmetrical on both sides of the preceding value and is bounded by two-phase regions, coexisting respectively with L_1 and L_2.

TABLE I. Direct and reversed mesosphases in the binary phase diagrams of lyotropic systems. The notation of Ekwall [11] is used for the mesophases.

Binary system	Sequence of mesophases	Ref.
Aerosol OT-water (100 °C)	W L_1 D I_2' L_2 M	c
	1/2	
Triton X-100-water (20 °C)	W L_1 ? E ? L_2 M	a
	1/2	
Emu 09-water (20 °C)	W L_1 E D L_2 M	b
	1/2	
Emu 02-water (20 °C)	W L_1 D L_2 M	b
	1/2	
Decaoxyethylene glycol monolauryl ether-water (20 °C)	W L_1 I_1'' E L_2 M	a
	1/2	

[a]P. Ekwall, L. Mandell, and K. Fontell, Mol. Cryst. Liquid Cryst. **8**, 157 (1969).
[b]S. Friberg, L. Mandell, and K. Fontell, Acta Chem. Scand. **23**, 1055 (1969).
[c]J. Rogers and P. A. Winsor, J. Colloid Interace. Sci. **30**, 247 (1969).

It appears from Table I that a change of curvature of the interfaces, which is necessary following our description for the stabilization of direct and reversed ordered mesophases in the same system, has not been observed in a binary system, as it was already noted by Eckwall [11]. The possibility of realizing such a change is considerably improved if a third appropriate component is added to the amphiphilic-water system. Table II clearly illustrates this property since nine of the listed systems possess simultaneously in their ternary phase diagrams direct and reversed mesophases. In the table the systems have been divided into four groups.

Group A. This group includes the systems that possess in their phase diagram both the direct (E) and reversed (F) hexagonal mesophases. When the additional solute is an alcohol or a fatty acid, which are hydrophilic compounds, it has the effect of removing the L_1 and L_2 regions in the water-rich and solute-rich corners of the triangular phase diagrams, respectively. The action of the solute transforms the symmetric location of the direct and reversed phases with respect to the middle ($c=\frac{1}{2}$) of the water-association-colloid triangle side onto a symmetry with respect to the mediator of the triangle passing by the solute vertex (i.e., the actual symmetry with respect to the axis $c=\frac{1}{2}$ is lost). One can verify this property for the six systems listed at the top of Table II: The E and F phases are found to be approximately centered on the preceding axis for low and high contents of the solute. The shape of these phases is almost symmetrical with respect to the same axis, for the systems containing decanol or nonanol, reflecting the influence of the F symmetry. By contrast, when the solute is a fatty acid the shapes of E and F are disymmetrical, denoting F-noninvariant systems. In the decaoxyethilene glycol–water system the symmetry with respect to the mediator of the triangle holds also for the direct (I_1') and reversed (I_2''') cubic phases for low and middle contents of oleic acid, respectively.

Group B. The same sequences of direct phases as in the phase diagrams of the systems belonging to group A are found, but the corresponding reversed phases (F or I_2'') are absent. It denotes a strong spontaneous curvature of the interfaces that cannot be inversed. This can be viewed, for instance, in the example of potassium-caprate-water-octanol, where the C phase is absent from the L_1-B-C-E sequence, found in the sodium caprylate system, while its reversed K analog appears.

Group C. The four systems pertaining to this group possess the particularity that the regions L_1 and L_2 form a single region L extending from pure water to pure solute in which one goes continuously from micelles of the direct type to micelles of the reversed type. It corresponds to the situation assumed in our approach for F-invariant systems, in which one finds direct and reversed mesophases within the same sequence.

Group D. The phase diagrams of the systems listed for the D systems in Table II confirm the interpretation given for F-noninvariant systems and the strong influence of the areas occupied by the L_1 and L_2 phases in the phase diagram on the stabilization of direct or reversed phases. Thus one has either a sequence of direct mesophases when the L_1 region occupies a large area in the phase diagram or a sequence of reversed mesophase when the L_2 region is predominant. The spontaneous curvature of the interfaces is opposed in the two preceding types of systems and the change in curvature, which would allow the existence of both types of mesophases, cannot be obtained by adding a solute.

Therefore, the analysis of the ternary phase diagrams that have been worked out in lyotropic systems allows one to

TABLE II. Direct and reversed mesophases in the ternary phase diagrams of lyotropic systems. The notation of Ekwall [11] is used for the mesophases.

	Ternary systems	Direct mesophases	Lamellar phase	Reversed mesophases	Refs.
A	Sodium caprylate-water + decanol	L_1-B-C-E		L_2-F	a,b
	Sodium caprylate-water + nonanol				c,d
	Sodium caprylate-water + caprylic acid				d,e,f
	Potassium caprylate-water + decanol				g
	Decaoxyethylene glycol monolaurly ether-water +oleic acid	L_1-B-CI_1'-E	D	L_2-I_2'''-F	c,f
	Potassium oleate-water + decanol	L_1-B-E-R			g
	Octylammonium chloride-water + p-xylene	L_1-E		F	f
B	Sodium caprylate-water + octanol	L_1-B-C-E		L_2	c
	Sodium caprylate-water + heptanol				d
	Sodium caprylate-water + hexanol				d
	Octyl ammonium cloride-water + decanol			L_2-I_2'''	f
	Potassium caprate-water + octanol	L_1-B-E		L_2-K	g
	Octyldimethyl ammonium chloride-water + decanol	L_1-I_1'-E	D		f
	Octyltrimethyl ammonium chloride-water + decanol				f
	Decaoxyethyleneglycol monolauryl ether-water +caprylic acid	L_1-I_1''-E		L_2	c,f
	Potassium oleate-water + p-xylene	L_1-R-E			c,d
	Cetyltrimethyl ammonium bromide-water +hexanol	L_1-E			f,h
C	Sodium caprylate-water + butanol	L_1-E	D	L	d
	Sodium caprylate-water +methanol				
	Sodium caprylate-water + propanol	L_1-I_1''-E	D		
	Sodium caprylate-water + ethanol				
D	Triton X-100-water + decanol	L_1-E		L_2	c,f
	Triton X-100-water + oleic acid	L-B-E			
	Emu 09-water + p-xylene				i
	Emu 09-water + hexadecane	L_1-I_1'-I_1''-E	D		
	Emu 02-water + p-xylene	L_1		L_2-F	j,k
	Aerosol OT-water + caprylic acid				
	Aerosol OT-water + decanol			L_2-I_2-F	
	Aerosol OT-water + p-xylene				j

[a]P. Ekwall, I. Danielson, and L Mandell, Kolloid Z. **169**, 113 (1960).
[b]L. Mandell and P. Ekwall, Acta. Polytech. Scand. Chem. **74**, 1 (1968).
[c]P. Ekwall, L. Mandell, and K. Fontell, Mol. Cryst. Liq. Cryst. **157**, 8 (1964).
[d]P. Ekwall, Advances in Liq. Crystals, Ed. G. Brown (Academic Press, NY 1975), Vol. 1, p. 1.
[e]P. Ekwall, S. Wiss, Friedrich-Schiller Univ. **14**, 181 (1965).
[f]P. Ekwall and L. Mandell, Kolloid Z. **233**, 938 (1969).
[g]P. Ekwall, L. Mandell, and K. Fontell, J. Colloid Interfaces Sci. **31**, 508 (1969).
[h]P. Ekwall, L. Mandell, and Fontell, J. Colloid Interfaces Sci. **29**, 639 (1969).
[i]S. Friberg, L. Mandell, and K. Fontell, Acta Chem. Scand. **23**, 1055 (1969).
[j]P. Ekwall, L. Mandell, and K. Fontell, J. Colloid Interfaces **33**, 215 (1970).
[k]K. Fontell, J. Colloid Interface Sci. **43**, 156 (1973).

disclose three main classes of phase diagrams. In the first class the L_1 and L_2 micellar solutions occupy equivalent areas of the phase diagrams. In this case the direct and reversed mesophases may both take place. They are located symmetrically with respect to the axis passing by the middle of the amphiphile-water side of the phase diagram triangle and by the solute apex. The direct and reversed phases can be symmetrically or nonsymmetrically shaped with respect to

the preceding axis. The second class of phase diagrams corresponds to the existence of a single micellar solution L with a continuous crossover between the direct and reversed micelles. Here the area occupied by the lamellar phase is considerably reduced and one may expect that direct and reversed ordered mesophases occur within the same sequence along the L phase. In the third class of phase diagrams one of the L_1 or L_2 micellar solution regions is predominant. Correspondingly, one will find either direct or reversed mesophases, but not both simultaneously.

VI. CONCLUSION

In summary, a general phenomenological approach to reconstructive phase transitions in lyotropic complex fluids has been proposed. The approach stresses the importance of reversed mesophases for understanding the underlying symmetries of such systems and the structure of the corresponding order-parameter space. It gives a description of the possible symmetries of ordered mesophases and of the general properties of the phase diagrams of lyotropic systems and it predicts the existence of new types of mesophases.

ACKNOWLEDGMENT

Fundação de Amparo à Pesquisa do Estado de São Paulo partially supported this work.

APPENDIX

The wave vector of the planar tetragonal Brillouin zone associated with the periodicity assumed for the undulation along x and/or y is $\vec{k}_1=(2\pi/a,0)$. Its invariance group is $C_s=\{c_1,\sigma_y\}$; thus, with respect to the product group $G_0=C_{4v}\otimes\Re^2$ assumed for the parent phase, the star k_1^* has four branches $\vec{k}_1,\vec{k}_2=(0,2\pi/a)$, $\vec{k}_3=-\vec{k}_1$, and $\vec{k}_4=-\vec{k}_2$, which are obtained by the symmetry operations C_1, C_4, C_2, and C_4^3, respectively. The little group C_s possesses two irreducible representations (IR's) denoted Γ_1 (the identity IR) and Γ_2, which correspond to a character -1 for σ_z. Note that Γ_1 and Γ_2 have, respectively, the transformation properties of a scalar and of an axial vector since one has, for their respective bases (φ_1,φ_2), $\sigma_z(\varphi_1)=\varphi_1$ and $\sigma_z(\varphi_2)=-(\varphi_2)$.

The 4×4 matrices generating Γ_1 and Γ_2 can be constructed using the procedure described in Ref. [22]. One finds for Γ_1

$$\hat{\sigma}_y=\begin{pmatrix}0&0&0&1\\0&0&1&0\\0&1&0&0\\1&0&0&0\end{pmatrix}, \tag{A1}$$

$$\hat{C}_4=\begin{pmatrix}1&0&0&0\\0&0&0&1\\0&0&1&0\\0&1&0&0\end{pmatrix},$$

$$\hat{t}=\begin{pmatrix}e^{i\vec{k}_1\cdot\vec{t}}&0&0&0\\0&e^{i\vec{k}_2\cdot\vec{t}}&0&0\\0&0&e^{i\vec{k}_3\cdot\vec{t}}&0\\0&0&0&e^{i\vec{k}_4\cdot\vec{t}}\end{pmatrix},$$

where $\vec{t}$ denotes a translation in the (x,y) plane. The matrices generating Γ_2 differ only from those of Γ_1 by the generating matrix

$$\hat{\sigma}_y=\begin{pmatrix}0&0&0&-1\\0&0&-1&0\\0&-1&0&0\\-1&0&0&0\end{pmatrix}.$$

Using the standard projector techniques given in Ref. [22], one obtains by applying the matrices associated with Γ_1 or Γ_2 to the four-component order parameter $(\Psi_{10},\Psi_{01},\Psi_{\bar{1}0},\Psi_{0\bar{1}})$, the invariants (rational basis of integrity)

$$I_1=\Psi_{10}\Psi_{\bar{1}0}+\Psi_{01}\Psi_{0\bar{1}},\quad I_2=\Psi_{10}\Psi_{\bar{1}0}\Psi_{01}\Psi_{0\bar{1}}.$$

Writing $\Psi_{10}=\rho_1e^{i\theta_1}$, $\Psi_{01}=\rho_2e^{i\theta_2}$, $\Psi_{\bar{1}0}=\Psi_{10}^*$, and $\Psi_{0\bar{1}}=\Psi_{01}^*$, one gets $I_1=\rho_1^2+\rho_2^2$ and $I_2=\rho_1^2\rho_2^2$.

[1] P.G. de Gennes, Phys. Lett. **30A**, 454 (1969).
[2] L.J. Yu and A. Saupe, Phys. Rev. Lett. **45**, 1000 (1980).
[3] P. Tolédano and A.M. Figueiredo Neto, Phys. Rev. Lett. **73**, 2216 (1994).
[4] J. Charvolin and P. Rigny, J. Chem. Phys. **58**, 3999 (1973).
[5] J. Charvolin, in *Liquids at Interfaces*, edited by J.F. Joanny and J. Zinn-Justin (Elsevier, Amsterdam, 1989), pp. 182–207.
[6] *Polymer Liquid Crystals*, edited by A. Ciferri, W.R. Krigbaum, and R.B. Meyer (Academic, New York, 1982).
[7] D.A. Hajduk *et al.*, Macromolecules **27**, 490 (1994).
[8] *Physics of Amphiphiles, Micelles and Microemulsions*, edited by V. Degiorgio and M. Corti (Academic, New York, 1985).
[9] *Physics of Amphiphilic Layers*, edited by J. Meunier, D. Langevin, and N. Boccara (Springer-Verlag, Berlin, 1987).
[10] D. Chapman, in *Advances in Liquid Crystals*, edited by G.H. Brown (Academic, New York, 1981), Vol. 5, pp. 1–45.
[11] P. Ekwall, in *Advances in Liquid Crystals*, edited by G.H. Brown (Academic, New York, 1975), Vol. 1, pp. 1–142.
[12] P.A. Winsor, Chem. Rev. **68**, 1 (1968).
[13] D. Andelman, M.M. Koztov, and W. Helfrich, Europhys. Lett. **25**, 231 (1994).
[14] K. Chen, C. Jayaprakash, R. Pandit, and W. Wenzel, Phys. Rev. Lett. **65**, 2736 (1990).
[15] M.E. Cates and S.T. Milner, Phys. Rev. Lett. **62**, 1856 (1989).
[16] S. Leibler and D. Andelman, J. Phys. (France) **48**, 2013 (1987).

[17] W. Helfrich, J. Phys.: Condens. Matter **6**, A79 (1994).
[18] G. Gomper and J. Gooss, Phys. Rev. E **50**, 1325 (1994).
[19] J. Meunier, in *Physics of Amphiphilic Layers* (Ref. [9]), p. 118.
[20] D. Roux and C.R. Safinya, in *Physics of Amphiphilic Layers* (Ref. [9]), p. 138.
[21] D.C. Morse, Phys. Rev. E **50**, R2423 (1994).
[22] J.C. Tolédano, and P. Tolédano, *The Landau Theory of Phase Transitions* (World Scientific, Singapore, 1987), Chap. 2.
[23] P.G. de Gennes, *Scaling Concepts in Polymer Physics* (Cornell University Press, Ithaca, 1979), p. 105.
[24] I.E. Dzialoshinskii, Zh. Éksp. Teor. Fiz. **46**, 1420 (1964) [Sov. Phys. JETP **19**, 960 (1964)].
[25] G.S. Smith, E.B. Sirota, C.R. Safinya, and N.A. Clark, Phys. Rev. Lett. **60**, 813 (1988).
[26] D.C. Wack and W.W. Webb, Phys. Rev. Lett. **61**, 1210 (1988).
[27] M.P. Hentschel and F. Rustichelli, Phys. Rev. Lett. **66**, 903 (1991).
[28] B. Mettout, P. Tolédano, H. Vasseur, and A.M. Figueiredo Neto, Phys. Rev. Lett. **78**, 3483 (1997).
[29] B. Mettout, P. Tolédano, H. Vasseur, E. A. Oliveira, and A. M. Figueiredo Neto, Phys. Rev. E (to be published).